

The Analysis of Radial/Axial Error Motion on a Precision Rotation Stage

Jinho Kim, Dongik Shin, Deokwon Yun, and Changsoo Han

Abstract—Rotating stages in semiconductor, display industry and many other fields require challenging accuracy to perform their functions properly. Especially, Axis of rotation error on rotary system is significant; such as the spindle error motion of the aligner, wire bonder and inspector machine which result in the poor state of manufactured goods. To evaluate and improve the performance of such precision rotary stage, unessential movements on the other 5 degrees of freedom of the rotary stage must be measured and analyzed. In this paper, we have measured the three translations and two tilt motions of a rotating stage with high precision capacitive sensors. To obtain the radial error motion from T.I.R (Total Indicated Reading) of radial direction, we have used Donaldson's reversal technique. And the axial components of the spindle tilt error motion can be obtained accurately from the axial direction outputs of sensors by Estler face motion reversal technique. Further more we have defined and measured the sensitivity of positioning error to the five error motions.

Keywords—Donaldson's reversal methods, Estler face motion reversal method, Error motion, sensitivity, T.I.R (Total Indicated Reading).

I. INTRODUCTION

IN many high-precision machines, instruments of semiconductor manufacturing and display industry require challenging accuracy to perform their functions properly. Especially, Axis of rotation error on rotary system is significant; such as the spindle error motion of the aligner, wire bonder, and inspector machine which result in the poor state of manufactured goods. To evaluate and improve the performance of such precision rotary stage, unessential movements on the other 5 degrees of freedom (3-Translation, 2-Tilt) of the rotary stage must be measured and analyzed. Unessential movements are typically measured by displacement measuring sensors to a high precision sphere or cylinder. Output data of sensors include profile error, centering error, and error motion. Over the years, several separation techniques have been developed for the accurate measurement of profile error to error motion, such as the Donaldson's reversal method [1,2], the multi-step method [3], and the multi-probe method [4, 5]. Review of these techniques is given in [6]. And the Estler face motion reversal method is introduced that allows the separation of tilt and axial error motions from the circular flatness of a reference part [7].

Authors are with the Mechanical Engineering Department, Hanyang University, Sa-1 dong, Sangrok-gu, Ansan-si, Gyunggi-do, 426-791, Korea (the corresponding author to provide phone: 82(0)11-9179-6253; fax: 82(0)31-406-6398; e-mail: jjiropunch@gmail.com, e-mails of other authors: sdongik@gmail.com, enoch@hanyang.ac.kr, cshan@hanyang.ac.kr).

ANSI/ASME specified the error motion of an axis of rotation and measurement method in 1986 and revised in 1995 [8]. This specification was fueled mainly by industry of machine tools, coordinate machines, and so on. In this paper, we have measured the three translations and two tilt motions of a rotating stage with high precision capacitive sensors. Further more we have defined and measured the sensitivity of positioning error to the five error motions.

II. THEORETICAL ANALYSIS

When a probe measures the movement of a rotating target, the raw measurement data is defined as "the total displacement measured by an instrument sensing against a moving surface or moved with respect to a fixed surface." in ANSI/ASME[8]. And it is called the runout or T.I.R (Total Indicated Reading). In contrast, radial error motion is positioning error of the changes in position, relative to the reference coordinate axes. Radial runout will be identical to radial error motion only if both of roundness error and centering error are removed. It is traditionally illustrated as a function of the spindle's angular position using a polar plot. For example, Fig.1 shows polar plot of the synchronous and asynchronous components of radial error motion from 100 revolutions with 100 rpm of a test module system.

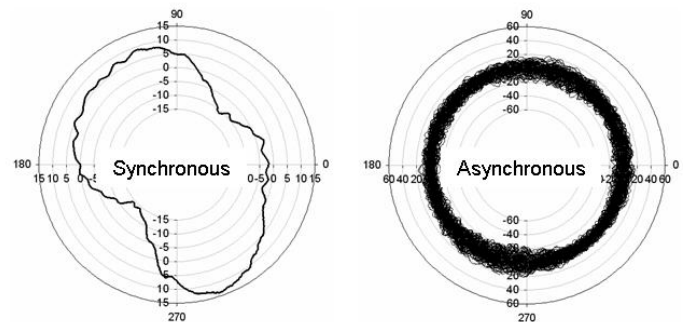


Fig. 1 Synchronous and Asynchronous radial error motion of spindle driven by PZT

To obtain error motion values, a computer-based measurement system allows the analyst to:

1. Eliminate the once-per-revolution component from radial measurements.

2. Eliminate very low frequency variations to compensate for thermal drift.
3. Perform an error separation technique to distinguish the profile error from the spindle error motion.

A. RRO (Repeatable RunOut) vs. NRRO (Non-Repeatable RunOut)

The signal obtained from the capacitance sensor is proportional to the radial displacement of the spindles. This signal called total indicated reading (T.I.R), is the sum of a profile error, eccentricity, error motion components, and a non-repeatable components. Non-repeatable value reflects the influence of the spindle plus environmental disturbances, structural vibration, and electrical noise so that T.I.R can be written as follows.

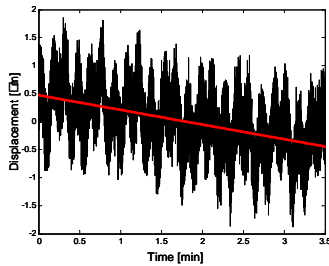
$$T.I.R(t) = RRO(t) + NRRO(t) \quad (1)$$

The RRO (Repeatable RunOut) is computed by taking average of the T.I.R (signal data) from N revolutions of the spindle at each of the angular measurement locations.

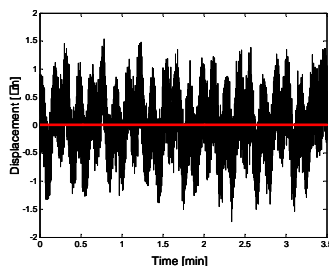
$$RRO(t) = \frac{1}{n} \sum_{i=1}^n TIR(t) \quad (2)$$

Substituting (2) into (1), NRRO can be obtained by subtracting RRO, i.e. the average of T.I.R, from T.I.R.

$$NRRO(t) = TIR(t) - RRO(t) \quad (3)$$



(a) Drift component data



(b) Elimination of drift component

Fig. 2 Drift component data and its elimination

B. Elimination of Once-Per-Revolution Component

An off-center in mechanical mounting and set-up error add an unwanted component to the spindle motion error. Those errors are a once-per-revolution sinusoidal wave in rectilinear coordinates and it must be eliminated in measurement data, even though these errors are very small. In this paper, the FFT (Fast Fourier Transform) and IFFT (Inverse Fast Fourier Transform) algorithms are used for eliminating fundamental component.

C. Elimination of Drift Component

Low frequency variations, like thermal drift and structural motion, which have periods exceeding the recording time of the spindle measurements, should be filtered from the measurements data. These low frequency variations do not necessarily have equal values at the beginning and end of the recorded data. Fig. 2 (a) shows the low-variation drift relative to the Z reference axis and a best fit, low order polynomial is removed from the data to reduce the influence of very low frequency disturbances in Fig. 2 (b).

D. Donaldson Reversal Method

The Donaldson reversal method, which is the rotational equivalent of the well-known straightedge reversal, is shown schematically in Fig. 3. The recorded value of $M_1(\theta)$ is the sum of the roundness profile $P(\theta)$ and radial error motion $S(\theta)$.

$$M_1(\theta) = P(\theta) + S(\theta) \quad (4)$$

Second recorded value of $M_2(\theta)$ is recorded, with the stage and indicator orientation rotated by 180° between measurements.

$$M_2(\theta) = P(\theta) - S(\theta) \quad (5)$$

This changes the sign of the stage's profile error within the two measurements, enabling the computation of the part profile $P(\theta)$ and spindle error motion $S(\theta)$ using the simple relations in (4), and (5).

$$P(\theta) = \frac{M_1(\theta) + M_2(\theta)}{2} \quad (6)$$

$$S(\theta) = \frac{M_1(\theta) - M_2(\theta)}{2} \quad (7)$$

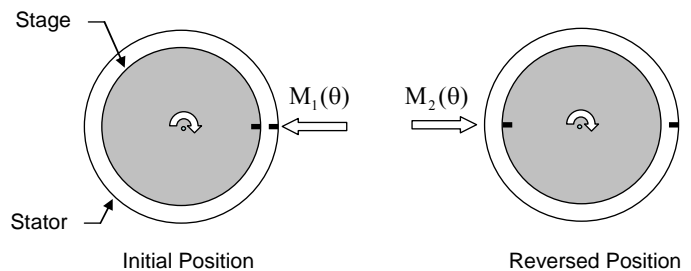


Fig. 3 Schematic of the Donaldson reversal method

E. Estler Face Reversal Technique

The Estler face reversal described in [7] uses two measurement setups similarity to Donaldson reversal method as shown in Fig. 4. The first setup is the initial position measurement which value is the sum of the circular flatness $F(\theta)$, axial error motion $A(\theta)$ and tilt error motion $T(\theta)$.

$$I_1(\theta) = F(\theta) + rT(\theta) + A(\theta) \tag{8}$$

In the second step, the reversal position, the measured stage and indicator are rotated 180° about the axis of rotation and relative to the first setup.

$$I_2(\theta) = F(\theta) - rT(\theta) + A(\theta) \tag{9}$$

The on-axis indicator in the second setup $I_4(\theta)$ is optional.

$$I_3(\theta) = I_4(\theta) = A(\theta) \tag{10}$$

From (8) ~ (10), axial and tilt error motion results in:

$$A(\theta) = \frac{I_3(\theta) + I_4(\theta)}{2} \tag{11}$$

$$T(\theta) = \frac{1}{r} \left(\frac{I_1(\theta) - I_2(\theta)}{2} - \frac{I_3(\theta) + I_4(\theta)}{2} \right) \tag{12}$$

And circular flatness is:

$$F(\theta) = \frac{I_1(\theta) + I_2(\theta)}{2} - \frac{I_3(\theta) + I_4(\theta)}{2} \tag{13}$$

Furthermore, the on-axis measurement is not directly involved with the reversal part of this technique but is still required for the analysis. This measurement, therefore, does not necessarily need to be done at the same time or on the same measured part as the normal and reversal measurements. This feature of the

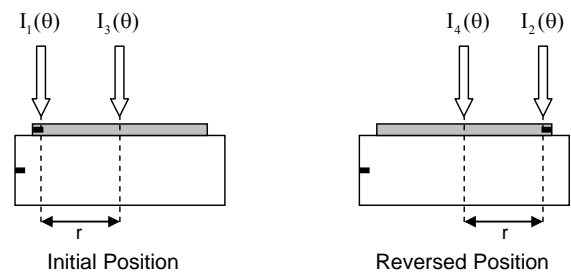


Fig. 4 Schematic of the Estler face motion reversal method

Estler face reversal differs for other common reversals, such as straightedge and Donaldson reversal, and presents some opportunities when reducing the technique.

III. ERROR MOTIONS AND POSITION ERROR

The error motions are displacements of axis. A perfect spindle provides 1 DOF rotational motion about a fixed axis, whereas the actual spindle cannot go without additional 5-DOF displacements of its axis of rotation: rotation angle θ_z , tilt error motion ϵ_x , and ϵ_y , radial error motion δ_x and δ_y and axial error motion δ_z . With attachment of a coordinate system, the positions of ideal and actual spindles can be represented by homogeneous transform matrix.

$$T_{ideal} = rot(\theta_z) \tag{14}$$

$$T_{actual} = tran(\delta_x, \delta_y, \delta_z) rot(\epsilon_x) rot(\epsilon_y) rot(\theta_z) \tag{15}$$

Note that the error motions are functions of the rotation angle. The positioning error of an arbitrary point on the spindle whose representation in spindle coordinate system is (16) can be defined as (17).

Open Science Index, Mechanical and Mechatronics Engineering Vol:1, No:5, 2007 publications.waset.org/2242.pdf

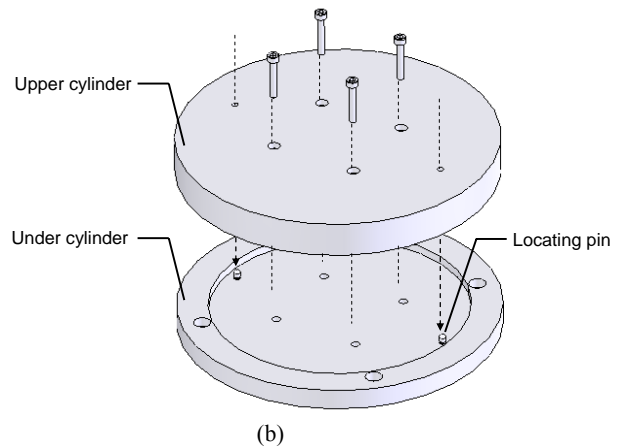
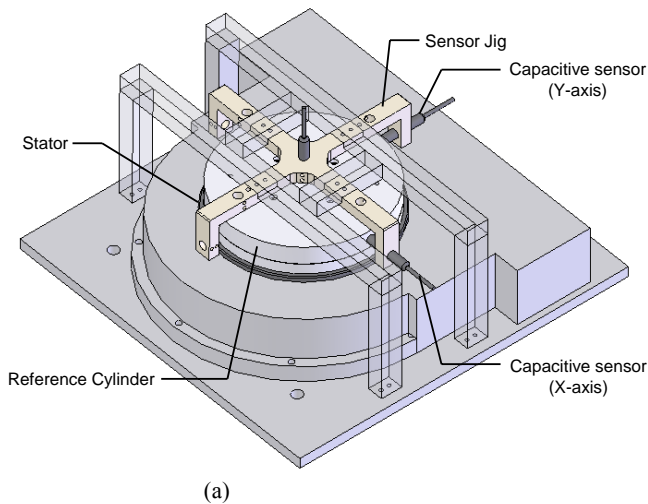


Fig.5 (a) Precision Stage and measurement system configuration, (b) The separated reference cylinder for reversal method

$$p = (r \cos \phi, r \sin \phi, z, 1) \quad (16)$$

$$e \equiv T_{actual} p - T_{ideal} p \quad (17)$$

Applying small angle approximation for tilt errors,

$$e \equiv \begin{bmatrix} z\varepsilon_Y + \delta_X \\ -z\varepsilon_X + \delta_Y \\ -r\varepsilon_Y C(\theta_Z + \phi) + r\varepsilon_X S(\theta_Z + \phi) + \delta_Z \end{bmatrix} \quad (18)$$

Sensitivities of positioning error e to the error motions δ_X , δ_Y , δ_Z , ε_X , and ε_Y are defined as

$$s_i \equiv \frac{de}{e} \bigg/ \frac{d\delta_i}{\delta_i} = \frac{\delta_i}{e} \frac{\partial e}{\partial \delta_i} \quad (19)$$

IV. EXPERIMENTAL SETUP

Displacement is measured by three capacitive sensors with 0.083mV-rms Noise (ADE Technologies with 2805-1probes). Each of the non-contact capacitance sensors can mount on the sensor mounting machine at 90 deg to each other and are typically aligned with the X, Y and Z axes of the machine in Fig. 5. These probes have a measuring range of $\pm 100\mu\text{m}$ and resolution inferior to 20nm. And noise levels are 0.83 nm. Displacement measurements were recorded during 10 revolutions of the rotor while rotating at a fixed speed of 0.7 rpm. A rotary encoder was attached to the spindle rotor and a reading from the displacement signal was triggered with each pulse from the rotary encoder, providing 36,000,000 counts per revolution. The analog output from the sensors is sampled by a 16 bit data acquisition board (dSpace). We have designed sensor mounting and artifact to easily execute the reversals (Fig. 5). The artifact is separable into base cylinder and upper cylinder and they are mated with pin for accuracy in the reversed configuration.

The rotating stage is driven by worm gear in the tangential direction of the stage.

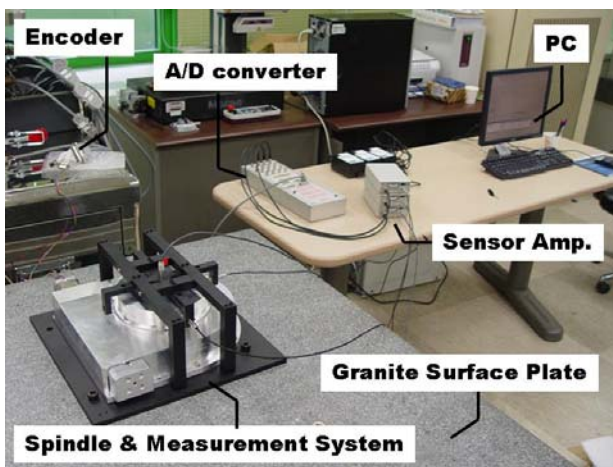
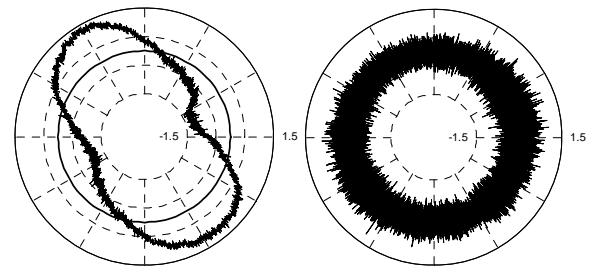
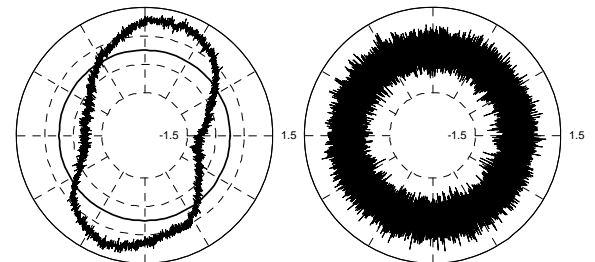


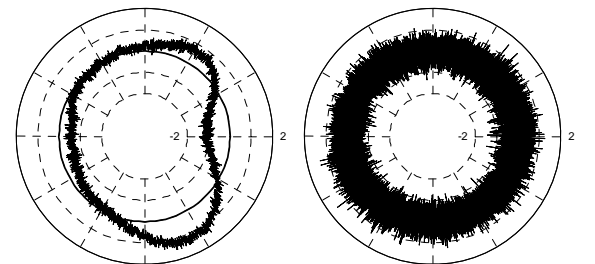
Fig. 6 Experimental Setup



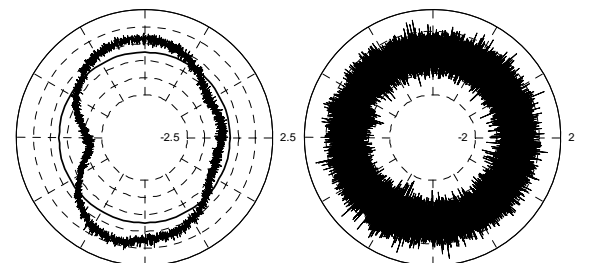
(a) Radial error motion (x-axis)



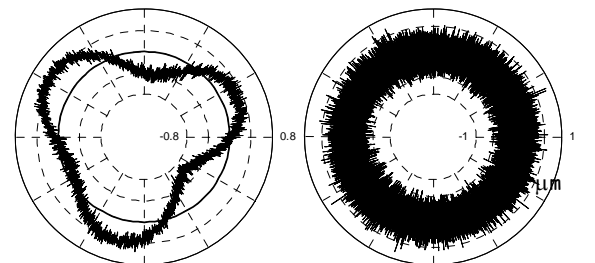
(b) Radial error motion (y-axis)



(c) Tilt error motion (x-axis)



(d) Tilt error motion (y-axis)



(e) Axial error motion

Fig. 7 Results of 5-DOF Synchronous and Asynchronous error motion polar plots

TABLE I
 MEASURED ERROR MOTION AND PROFILE ERROR

	Synchronous E.M*	Asynchronous E.M	Profile error
Radial x	2.87	3.12	2.37
Radial y	2.72	3.79	
Axial	1.38	1.61	-
Face x	2.99	3.03	7.30
Face y	3.79	3.51	
Tilt x	46.01	46.60	-
Tilt y	58.33	54.00	-

*E.M : Error Motion

Unit of Radial, Axial, Face error motion, and Profile error: μm

Unit of Tilt error motion: μrad

TABLE II
 MEASURED SENSITIVITY

Positioning error	Error motion	Sensitivity	
		Sync.	Async.
e_x	δ_x	1.46	2.79
	ε_y	1.06	2.45
e_y	δ_y	6.43	2.55
	ε_x	5.66	2.07
e_z	δ_z	2.28	3.84
	ε_x	2.12	3.92
	ε_y	1.48	4.17

Sync.: Synchronous component

Async. Asynchronous component

V. EXPERIMENTAL RESULT

Table I and Fig. 7 show the measured error motion values and form errors. The face motions at radius 65mm caused by tilt error are given to intuitive comparison of tilt error to displacement error. Table II represents sensitivities of positioning error of the point $p=(65\text{mm}, 0\text{ rad}, 27\text{mm})$ with respect to the measured error motion. These values are averaged over entire revolution.

We can conclude the y-direction error (perpendicular to the direction of motor drive) is relatively easy to reduce, improvement should be focused on the reduction of δY and εX .

VI. CONCLUSION

We identified the error motions of an axis of rotation and modeled the positioning error of a rotating stage with these error motions. We have measured the runout of the stage and extract the error motion for the rotating axis with several algorithms. Finally we analyzed the sensitivity of the target system

REFERENCES

- [1] Donaldson, R.R., "A Simple Method for Separating Spindle Error from Test Ball Roundness Error.", CIRP-Annals., Vol. 21, No. 1, pp.125-126., 1972.
- [2] Evans, C. J., Hocken, R. J., Estler, W. T, *Self- calibration: reversal, redundancy, error separation, and absolute testing.* CIRP Annals, Vol. 45, No. 2, pp. 483-492, 1996.
- [3] Spragg, R., and Whitehouse, D., procedures of the Institute of Mechanical Engineers, 182, 1968.

- [4] Grejda, R.D., "Use and Calibration of Ultraprecision Axes of Rotation With Nanometer Level Metrology", in *Mechanical Engineering*. 2002, The Pennsylvania State University, p.135.
- [5] Whitehouse DJ. "Some Theoretical Aspects of Error Separation Techniques in Surface Metrology", J. of Phys. E:Sci.Inst., Vol. 9, pp. 531-536, 1976.
- [6] Marsh E., Couey J., and Vallance R., "Nanometer Lever Comparison of Three Spindle Error Motion Separation Techniques."
- [7] James G.Salsbury., "Implementation of the Estler face motion reversal technique.", *Precision Engineering*, Vol.27, pp.189-194, 2003.
- [8] ANSI B89.3.4, "Axes of Rotation: Methods for Specifying and Testing Standard", ANSI/ASME, 2004.